ARMA 16-320

SAND2016-1777C

Implementation of a Full-Dome, Sonar-Based Finite Element Geomechanical Model to Analyze Cavern and Well Stability at the West Hackberry SPR Site

Sobolik, S.R.

Sandia National Laboratories, Albuquerque, New Mexico, USA

ABSTRACT: This report presents computational analyses that simulate the structural response of crude oil storage caverns at the U.S. Strategic Petroleum Reserve (SPR) West Hackberry site in Louisiana. These analyses evaluate the geomechanical behavior of the 22 caverns at the West Hackberry SPR site for the current condition of the caverns and their wellbores, the effect of the caverns on surface facilities, and for potential enlargement in the form of drawdowns. These analyses represent a significant upgrade in modeling capability, as the following enhancements have been developed: a 6-million finite element model of the complete West Hackberry dome; cavern finite element mesh geometries fit to sonar measurements of those caverns; the full implementation of the multi-mechanism deformation (M-D) creep model; and the use of historic wellhead pressures to analyze the past geomechanical behavior of the caverns. The analyses examined the overall performance of the West Hackberry site by evaluating surface subsidence, horizontal surface strains, and axial well strains. This report presents a case study of how large-scale computational analyses may be used in conjunction with site data to make recommendations for safe depressurization and repressurization of oil storage caverns with unusual geometries and close proximity, and for the determination of the number of available drawdowns for a particular cavern.

1. INTRODUCTION

The U.S. Strategic Petroleum Reserve (SPR), operated by the U.S. Department of Energy (DOE), stores crude oil in solution-mined caverns in the salt dome formations of the Gulf Coast. Until recently, there were a total of 62 caverns located at four different sites in Texas (Bryan Mound and Big Hill) and Louisiana (Bayou Choctaw and West Hackberry); within the past year, the SPR has decided to decommission West Hackberry Cavern 6 and Bryan Mound Cavern 2, reducing the number of SPR caverns to 60. Each cavern is constructed and then operated using casings inserted through a wellbore or wellbores that are lined with steel casings cemented in place from the surface to near the top of the cavern. The West Hackberry salt dome in the extreme southwestern corner of Louisiana, some 24 km from the Louisiana/ Texas border to the west and the Gulf of Mexico to the south. It has an oil storage capacity of about 35×10^6 m^3 (222×10^6 barrels) within 21 caverns, and has operated since 1980.

Since the SPR took ownership of the Phase 1 caverns in 1978, several finite element analyses have been performed to assess the long-term performance and stability of the caverns, each with increasing levels of constitutive model development and technical complexity. Early analyses [1] were conducted using two-dimensional axisymmetric idealizations and each cavern was simulated independently of the others. While the analyses at that time predicted stability, cavern workover conditions were not simulated. In 2002, computations used a 30-degree wedge to simulate a symmetric 19-cavern field geometry [2]. The caverns in that simulation were modeled as true cylinders. In 2009, a substantially upgraded computational analysis of West Hackberry was performed by using a three-dimensional computational domain that included twelve specific caverns and the eastern half of the salt dome [3]. The pre-SPR Phase 1 caverns were meshed with geometries based on sonar data measurements, whereas the SPR-constructed Phase 2 caverns were modeled as frustums of approximately equal volume, radii and height. For the 2009 analyses, the entire lives of the caverns (construction, brine or oil storage, operating and workover pressures) were modeled individually for each cavern, with average operating pressures and idealized five-year workover schedules applied to each cavern on a rotating basis. All of the aforementioned analyses modeled the salt creep behavior using the power law creep model, a simplified creep model that calculates the secondary steady state creep mechanism, a subset of the more complete multi-mechanism deformation (M-D) model of salt creep [4, 5, 6]. The implementation of the power law creep model included the use of a reduced elastic modulus to simulate the transient response of the

salt to pressure changes. The resulting simulations provided satisfactory predictions of long-term creep behavior, but not of transient response to pressure changes. Beginning in 2010, the 2009 model converted to using an improved implementation of the complete M-D model [7]. This model was then used with the half-dome computational mesh to analyze specific cavern operation concerns regarding West Hackberry Caverns 6, 8, and 9 [8, 9, 10].

This report presents the most recently improved computational analyses that simulate the structural response of caverns at the SPR West Hackberry site. The history of the caverns and their shapes are simulated in a three-dimensional geomechanics model of the site that predicts deformations, strains, and stresses. Future leaching scenarios corresponding to oil drawdowns using fresh water are also simulated by increasing the volume of the caverns. Cavern pressures are varied in the model to capture operational practices in the field. The results of the finite element model are interpreted to provide information on the current and future status of subsidence, well integrity, and cavern stability. These analyses represent a significant upgrade in modeling capability, as the following enhancements have been developed: a 6-million finite element model of the complete West Hackberry dome; cavern finite element mesh geometries fit to sonar measurements of those caverns; the full implementation of the multi-mechanism deformation (M-D) creep model; and the use of historic wellhead pressures to analyze the past geomechanical behavior of the caverns. The analyses examined the overall performance of the West Hackberry site by evaluating surface subsidence, horizontal surface strains, and axial well strains. This report presents a case study of how large-scale computational analyses may be used in conjunction with site data to make recommendations for safe depressurization and repressurization of oil storage caverns with unusual geometries and close proximity, and for the determination of the number of available drawdowns for a particular cavern.

2. ANALYTICAL ADVANCEMENTS

There are several important advances in this new computational simulation of the West Hackberry geomechanical site:

Advancement #1: Transition to Adagio: JAS3D [11], which is a three dimensional iterative solid mechanics code, has been used for the structural analyses for the SPR system since the 1990s. JAS3D is no longer supported by Sandia, and has been replaced by Adagio [12, 13]. Adagio is written for parallel computing environments, and its solvers allow for scalable solutions of very large problems. The Adagio structure is different from JAS3D. Adagio uses the SIERRA Framework, which allows for coupling with other SIERRA mechanics codes. A simulation was performed with Adagio to replicate the simulation using the half-dome model and the M-D creep constitutive model with JAS3D [7, 8]; the new results were compared with the previous JAS3D predictions for purposes of verification, and found to produce nearly equal results [14].

Advancement #2: Computational mesh enhancement: The West Hackberry model computational mesh has been enhanced to include the entire salt dome, all SPR caverns meshed to axisymmetric geometries based on sonar measurements, and for caverns 6 and 9, leaching layers based on results from the cavern leaching prediction tool SANSMIC [15].

Advancement #3: A new baseline set of simulations has been run using the new computational mesh. One important new feature is the use of historical cavern wellhead pressures to develop the evolution of cavern behavior to the present, i.e., late 2014.

3. SITE DESCRIPTION

The geological characteristics related to the West Hackberry site were first described by Whiting [16]. The updated three-dimensional models of Rautman et al. [17] used a more refined analysis of the data and produced models of the dome that differed slightly from the earlier models. The West Hackberry dome consists of the more-or-less typical geologic sequence of rocks. With increasing depth below the ground surface, initially there is roughly 480 m of soil and unconsolidated gravel, sand, and mud, followed by approximately 120 m of caprock, consisting of anhydrite and carbonate (a conversion product of anhydrite). Generally, the upper portions of the caprock consist of the anhydrite conversion products of gypsum and dolomite, while the lower portion of the caprock is the initial anhydrite residue from the solution of the original domal material. The caprock is generally lens-shaped, tapering to thin edges toward the periphery of the dome.

The West Hackberry site consists of 22 caverns. Figure 1 shows the relative locations and geometries of these caverns. SPR purchased five existing caverns in the early 1980s. These five Phase 1 caverns – Caverns 6, 7, 8, 9, and 11 – were created as early as 1946 and were used for brining and brine storage before the SPR took ownership of them in 1977. After that time, seventeen other storage caverns (numbered 101 to 117) were created over an eight-year period. The post-1981 caverns were built via solution mining, and all have a generally cylindrical shape (more specifically, frustums with the larger diameter at the top) of approximately 600 m (2000 feet) height and 30-45 m (100-150 feet) in radius. The Phase

1 caverns, however, were originally built for brine production, and thus they were constructed with less concern about the long-term stability of the cavern shape. Cavern 6 at the West Hackberry site has an unusual dish-like shape with a large rim around the circumference. The diameter of Cavern 6 at the ceiling ranges from 340 to 380 meters. It is also in close proximity to Cavern 9, an hourglass-shaped cavern.

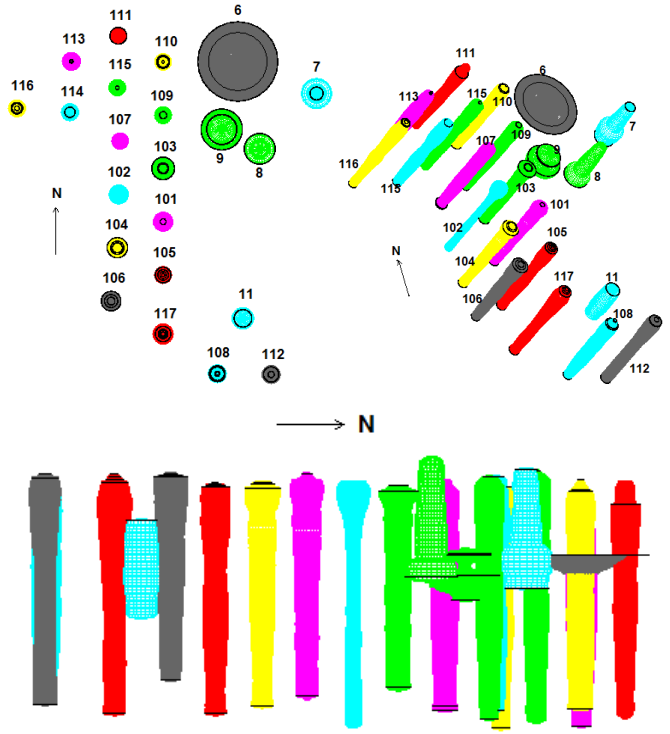

Fig. 1. West Hackberry caverns included in the computational mesh (3 views).

4. MODEL DESCRIPTION

The new full-dome computational model of the West Hackberry site has several enhancements over the previous analytical models. The intent of these enhancements is to compute stresses and strains using more accurate geometries of the salt dome and the caverns and their subsequent leaches, implement the M-D salt constitutive model with cavern-specific creep properties, and use the actual pressure histories to develop historical cavern behavior for evaluating future cavern drawdown availability. The analytical model follows the same general time history as previous analyses. The five caverns known as Phase 1 – Caverns 6, 7, 8, 9, and 11 – were created as early as 1946 and were used for brining and brine storage before the SPR took ownership of them in 1978. After that time, the seventeen Phase 2 storage caverns were created over an eight-year period. The simulation begins in 1945 with a one-year stress equilibration calculation. The analysis then simulates the creation of the Phase 1 caverns leached to full size over some period of time and filled with brine until 1981, and then filled with oil. The caverns are "created" by immediately removing the cavern material from the mesh by the element death option in Adagio, and at the same time applying a pressure boundary condition in the cavern that changes linearly from in situ salt pressure to cavern fluid pressure of the period of cavern creation. The analysis then simulates the creation of the post-1981 caverns and subsequent filling with oil. For periods before and after the available wellhead oil pressure histories, an average operating pressure with three-month workovers on five-year cycles is assumed. Drawdown, or leaching, operations to create additional volume are simulated periodically for a total of five drawdowns for all 22 caverns in five-year intervals beginning in 2018, and are done in a similar manner as the cavern creation.

The mesh for the computational model is illustrated in Figures 2 and 3. Figure 2 shows the entire mesh used for these calculations, and Figure 3 shows the same view with the overburden and caprock removed to expose the salt formation. The mesh comprises 5.99 million nodes and 5.95 million elements. Four material blocks are used in the model to describe the stratigraphic layers: the overburden, caprock, salt dome and sandstone surrounding the salt dome. The overburden is made of sand, and the caprock layer is made of gypsum and limestone. The overburden layer is 480 m thick, and the caprock is 120 m in the central portion of the dome. In an attempt to include the downward contour of the top of the salt dome at its outer perimeter, an outer ring of caprock has a total thickness of 240 m. Figure 4 superimposes the geometry of the West Hackbery dome obtained from seismic measurements onto the geometry created for the computational mesh, which was constructed by vertically extruding two palnar outlines of the salt dome boundary. The 22 SPR caverns are included in the mesh, as are three current Sempra natural gas storage caverns just to the west of the SPR site and three proposed cavern sites. Figure 5 shows the volume of WH-101 in both its computational mesh geometry and its oldest available sonar geometries from 2000 and 2006, and the geometries of the five drawdown layers built into the computational mesh. As is the case for all the Phase 2 caverns, the modeled drawdown layers extend for nearly the entire height of the cavern, and add approximately 15% to the volume of the cavern when they are removed.

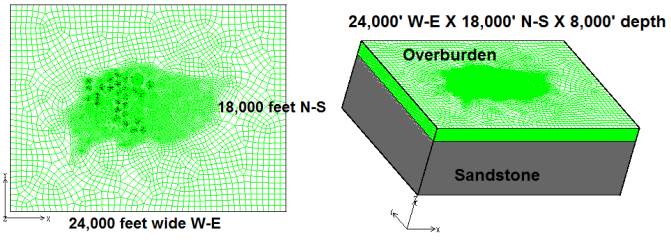

Fig. 2. Computational mesh,full-dome West Hackberry model.

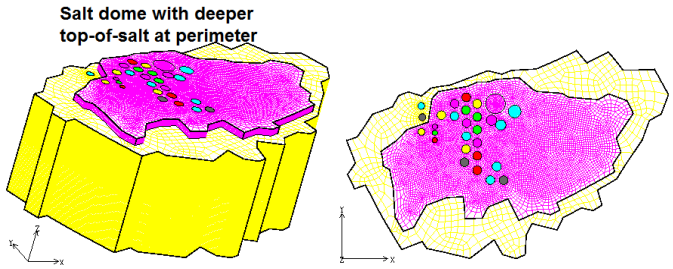

Fig. 3. Computational mesh showing the salt dome and cavern locations.

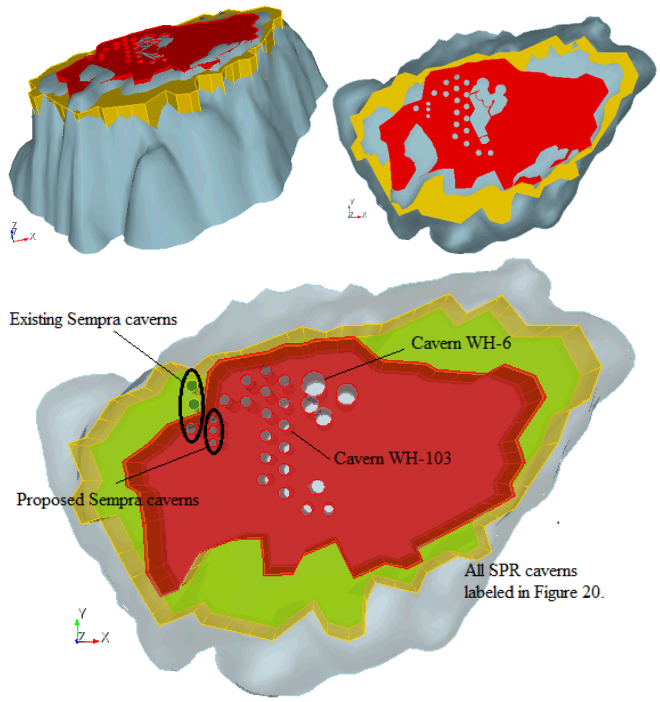

Fig. 4. Comparison of the salt dome geometry obtained from seismic measurements (grey) to the constructed salt dome for the West Hackberry geomechanical mesh (red and yellow).

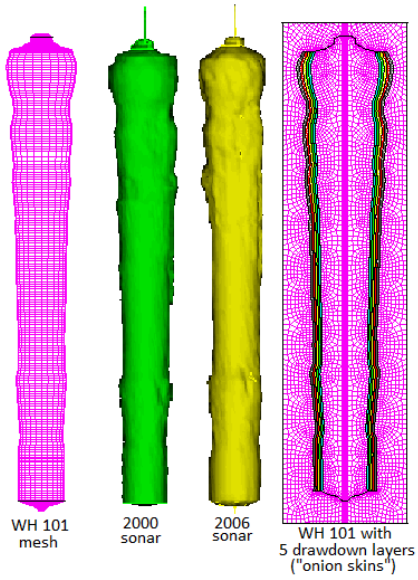

Fig. 5. Computational mesh, sonar geometries for WH-101.

WH Caverns 6 and 9 represent a significant challenge, both from a modeling standpoint and from an actual operational aspect as the cavern sizes increase along with the potential for adverse interactions. The meshes for these caverns are shown in Figure 6; the dimensions and relative locations of the caverns are shown to scale. The large rim around the bowl-like WH-6 was discovered from sonar and strapping data from the early 1980s. Previous computational analyses [3] determined that the upper and lower surfaces of the rim came into contact and essentially "closed" sometime in the mid-to-late 1990s; an analysis of the pressure and oil-brine interface data from WH-6 indicate the same conclusion happening in the early-to-mid 1990s. The inclusion of the open WH-6 rim in the computational simulations creates numerical instability in the calculation due to the initiation of contact algorithms when the top and bottom surfaces come into contact. The primary effects of the rim on any results of the calculations tend to be related to the behavior of the salt between WH-6 and 9, and not on any other caverns or on the overall subsidence of the site. Therefore, for the analyses presented in this report, the WH-6 rim volume and elements are not removed per element death as for the other caverns, but instead represented by salt with a smaller elastic modulus to allow it to deform more. The option to perform future calculations with the rim removed remains in the model.

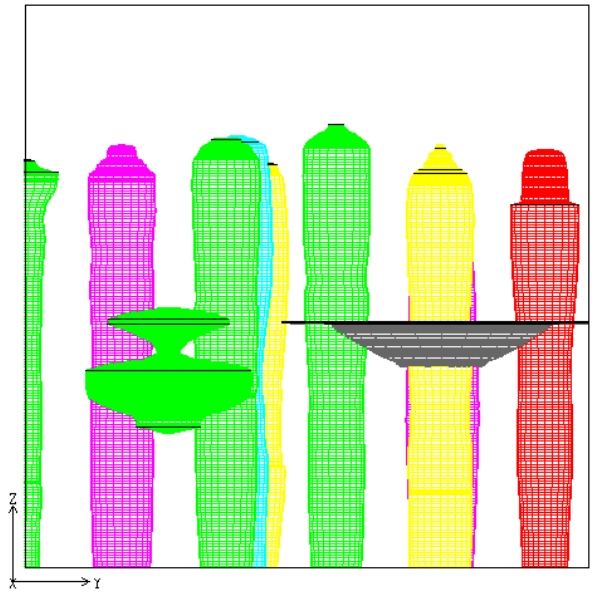

Fig. 6. Proximity of Caverns 6 (grey) and 9 (green).

In all of Sandia's previous geomechanical analyses of West Hackberry and the other SPR sites, approximated values for wellhead pressure (and thus, cavern pressure) based on general operating conditions have been used in the model. Both JAS3D and Adagio (because they are purely mechanical codes) require the specification of a pressure boundary condition on the inside of the cavern walls. The codes then predict cavern closure due to creep, but the cavern pressure does not automatically

change in the simulation. The historical wellhead pressure data for the cavern WH-101 are shown in Figure 7. The typical operating pressure range for the cavern is about 6.2-6.7 MPa (900-975 psi). As the cavern volume closes due to creep, the pressure increases for a period of time until some fluid is bled off at the wellhead; this bleed-off typically happens about every 90 days. Workover periods are observed to occur during those times when the wellhead pressure is near zero; mechanical integrity tests are represented by pressures significantly higher than 1000 psi. For previous SPR geomechanical analyses, this type of pressure history was represented by a constant wellhead operating pressure, with three-month workover period of zero pressure occurring every five years.

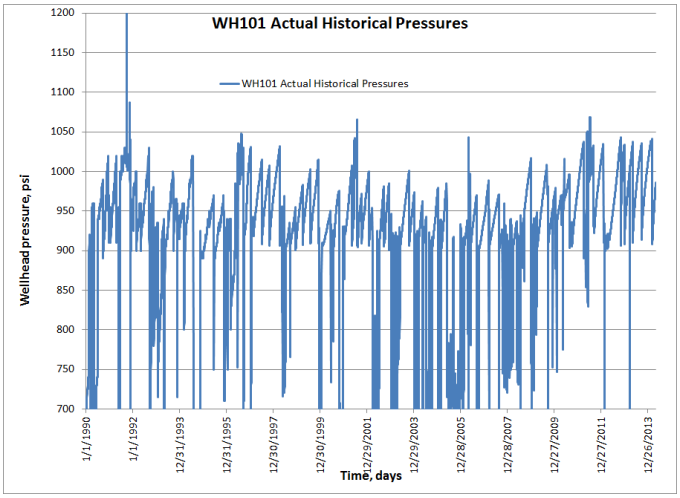

Fig. 7. Historical wellhead pressures for WH-101.

For this new geomechanical model for West Hackberry, it was decided to model the historical cavern pressure as closely as possible during the times when historical data are available. One of the reasons for doing this was to develop a better understanding of the creep behavior of caverns when an adjacent cavern is operated in workover mode. Examination of cavern wellhead pressure data indicate that when one cavern is in workover, the pressurization rate of adjacent caverns will increase [18]. This can be explained by the M-D creep model [4-6], which poses strain rate as a function of the equivalent stress, which is itself a measure of the magnitude of deviatoric stress. This deviatoric stress increases in the vicinity of a cavern when the fluid pressure is dropped to levels significantly less than the in situ stress. In previous SPR models, this increase in the pressurization rate has been observed as an increase in the cavern volume closure rate during a workover. One of the eventual goals of the new model is to use it to develop a predictive capability for monitoring pressurization rate changes in adjacent caverns, so as to help determine if leakage is occurring during these operations.

The classic M-D material properties for West Hackberry salt were based on laboratory data from core samples [19]; these properties are listed in Table 1. It was decided to run an initial simulation using the M-D properties in Table 1, and comparing the resulting predictions of cavern volume closure and surface subsidence to West Hackberry field data [14]. A reasonable agreement was achieved for surface subsidence, but the agreement for cavern closure was less satisfactory. To improve the predictions, it was decided to apply a multiplication factor to the secondary creep coefficient A_2. The cavern volume closure was used as the metric from which to derive multiplication factors, using the difference between least-square fit slopes to determine the factor. In addition, because of the variability of the discrepancies for each cavern, it was decided to apply individual factors to the region surrounding each cavern, as well as to the overall salt dome. Table 2 lists the secondary creep multiplication factors derived for each cavern and for the overall salt dome; these factors were used for the following model calculations.

Table 1. M-D Model mechanical properties published for West Hackberry salt [19].

Property	West Hackberry, soft salt properties
Density, lb/ft^3	144 (2300 kg/m^3)
Elastic modulus, lb/ft^2	648×10^6 (31.0 GPa)
Shear modulus G, lb/ft^2	259×10^6 (12.4 GPa)
Poisson's ratio	0.25
Primary Creep Constant A_1, sec^{-1}	9.81×10^{22}
Exponent n_1	5.5
Q_1, cal/mol	25000
Secondary Creep Constant A_2, sec^{-1}	1.13×10^{13}
Exponent n_2	5.0
Q_2, cal/mol	10000
B_1, sec^{-1}	7.121×10^6
B_2, sec^{-1}	3.55×10^{-2}
σ_0, , lb/ft^2	429×10^3 (20.57 MPa)
q	5335
m	3.0
K_0	6.275×10^5
c (1/R) (0.009198/1.8)	0.00511
α	-17.37
β	-7.738
δ	0.58
K_f, Multiplication factor for K_0 in Equation 11 (i.e., K_0 used in analysis = ($K_{0,\ Munson}$) * (K_f)	18.2

Table 2. Multiplication factors applied to the A_2 values listed in Table 1.

Cavern	A_2 multiplication factor	Cavern	A_2 multiplication factor
101	1.44	112	1.21
102	2.44	113	1.77
103	2.08	114	1.43
104	1.79	115	1.51

105	2.79	116	3.20
106	1.48	117	1.73
107	2.24	6	1.44
108	1.73	7	1.67
109	1.46	8	0.89
110	2.35	9	1.96
111	2.42	11	1.21
WH Salt	1.80		

5. ANALYSIS RESULTS

The historical performance of the West Hackberry caverns, and their predicted future performance, will be evaluated on the basis of several design factors: cavern volume closure, surface subsidence, dilatant and tensile stress damage to the salt surrounding the caverns, and axial well strain in the caprock. These performance factors will provide metrics to determine the long-term geomechanical performance of the caverns, and also the number of available drawdowns to expand the storage capacity of the caverns.

The volume of the caverns decreases as the salts creeps. The following figures compare the predicted cavern volume closure (as a percentage normalized by initial cavern volume) to those back-calculated from measured wellhead pressure data. Predicted cavern closure up to the present, and into the future, depends upon the timing of workover operations, during which the caverns undergo their greatest deformation, and of future cavern expansion (leaching) operations. Figure 8 shows the predicted and measured cumulative cavern closure for the Phase 1 caverns. In a similar fashion, Figures 9 and 10 present the cavern closure for the Phase 2 east side caverns and Phase 2 west side caverns. All of these figures show the amount of cavern closure from 1990 through 2014.

For the comparison between measured and predicted values, two immediate observations can be made. First, the slopes of the steady-state periods between workovers are still significantly different between measurements and predictions. This observation suggests that an increase of the magnitudes of the secondary creep coefficients may not be sufficient to match the measured closure rates. This result leads to at least one of the following conclusions: one, other M-D parameters, such as the primary creep coefficient A_1, or the primary and secondary creep exponents n_1 and n_2, may also need to be modified to provide a better match to the measured results; and two, the method used in the cavern pressure monitoring code CAVEMAN [20] to back-calculate the cavern volume closure may itself need to be reexamined to determine its correctness. The average difference between the predicted and measured cumulative percentage cavern volume closure in the period 1990-2014 is 21% over 22 caverns, which is an acceptable difference but one that still points to the opportunity for enhancing both the predictive methodology and the calculation of cavern volume loss from wellhead pressures.

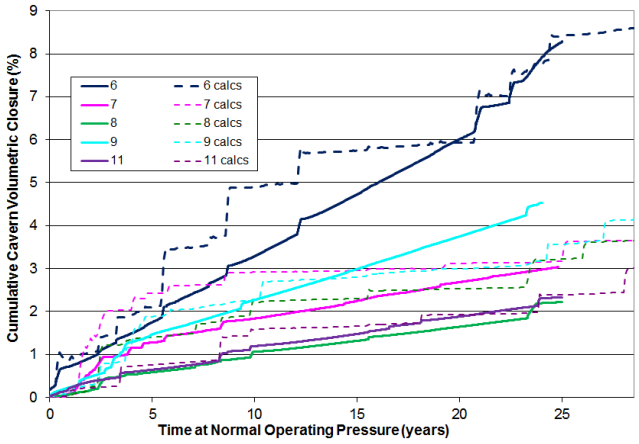

Fig. 8. Comparison between measured, predicted cumulative cavern volume closure since 1/1/1990 for West Hackberry Phase 1 caverns.

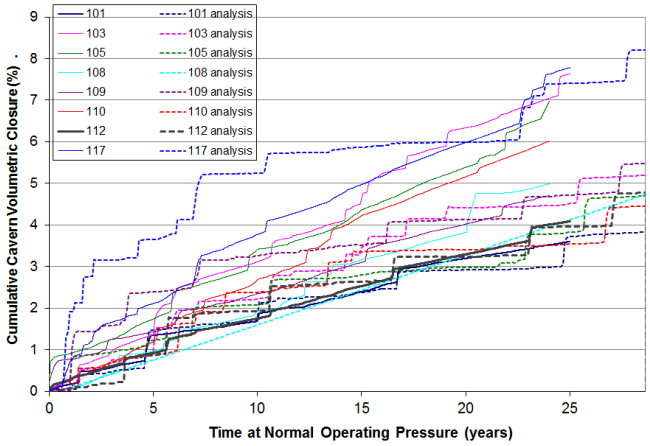

Fig. 9. Comparison between measured, predicted cumulative cavern volume closure since 1/1/1990 for West Hackberry Phase 2 caverns, east side.

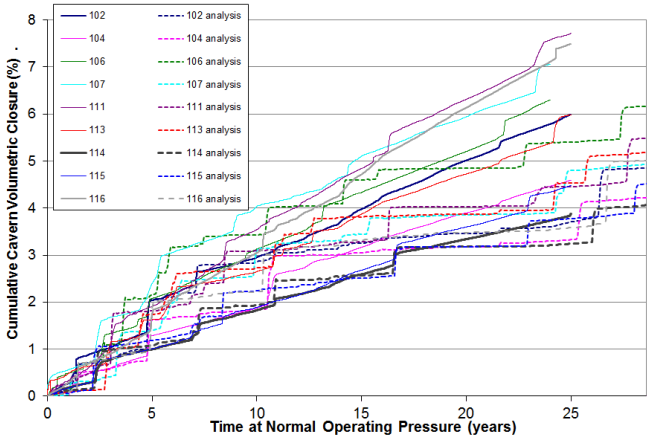

Fig. 10. Comparison between measured, predicted cumulative cavern volume closure since 1/1/1990 for West Hackberry Phase 2 caverns, west side.

The issue of surface subsidence is an important design and operations factor for surface facilities, especially for those located in flood prone areas, but subsidence also results in horizontal ground strains that can damage buildings, pipelines, and other infrastructure. The SPR is currently over 30 years old and the life of the SPR may extend another 30 years depending upon a number of factors, including oil consumption, import dependency, and geopolitical instability. Expected subsidence during a 100-year life of an SPR site on the order of up to 3 m (10 feet) is possible. Therefore, a reliable prediction of surface subsidence can be very valuable for site management. The plots in Figures 11 through 13 compare surface subsidence measured since 12/2/1982 to predicted values. Much like in the previous section, Figure 11 shows the predicted and measured surface subsidence above the Phase 1 caverns, and Figures 12 and 13 present the subsidence over the Phase 2 east side and west side caverns. The predictions tend to underpredict the surface subsidence over the caverns through 2014 by an average of 12%. The match is actually extremely good through 2006, after which the calculations exhibit a decrease in the rate of subsidence, whereas the data exhibit little if any significant change in their rate. It is unknown why the simulations predict this change in subsidence rate when the measurement do not; there may be other factors, such as regional subsidence, inelastic mechanics of the overburden, or uncaptured creep behavior, that are not adequately addressed in the model. Another interesting observation is that the predictions for subsidence over the Phase 1 and Phase 2 east side caverns seem match the data better than those for the Phase 2 west side caverns; this may be due to the operation of the Sempra caverns.

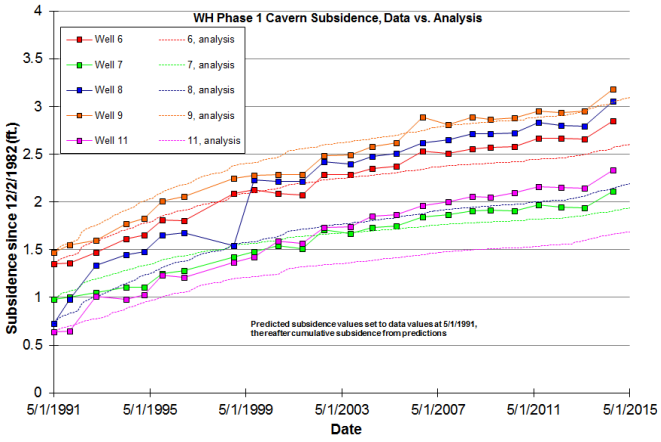

Fig. 11. Comparison between measured, predicted surface subsidence for West Hackberry Phase 1 caverns.

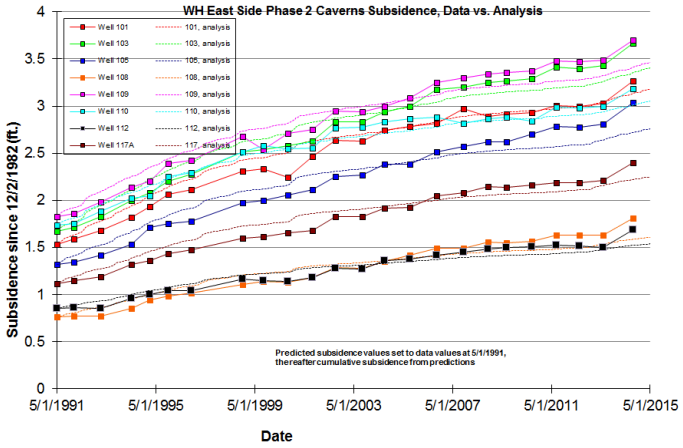

Fig. 12. Comparison between measured, predicted surface subsidence for West Hackberry Phase 2 caverns, east side.

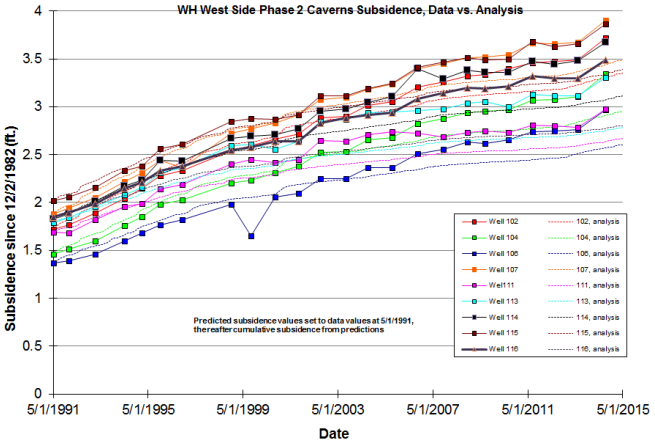

Fig. 13. Comparison between measured, predicted surface subsidence for West Hackberry Phase 2 caverns, west side.

Figure 14 shows predicted surface displacement with the assumed workover and cavern expansion cycles out to the year 2044 (when the facility is approximately 60 years old). The predictions indicate surface subsidence of an additional meter between 2014 and 2044, to a maximum of nearly 2 m (7 feet) since 1991. Because the surface structures at the wellhead are at elevations between 4 and 18 feet above sea level, the predicted subsidence may cause some of the wellheads to sink below sea level by the 2030s.

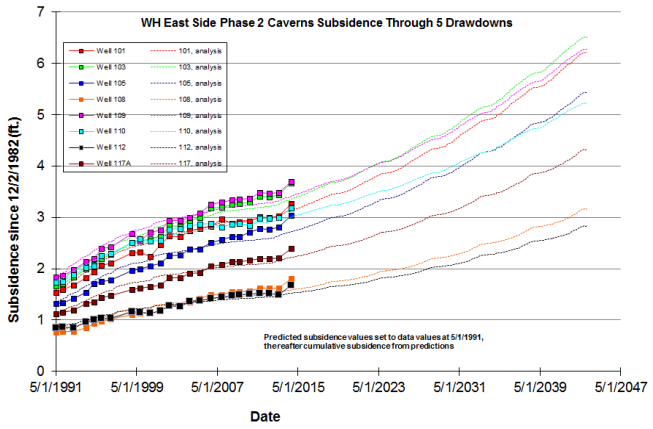

Fig. 14. Predicted subsidence over the Phase 2 east side caverns through 5 cavern drawdowns, to 2044.

There are two ways in which the salt surrounding the caverns can be damaged: by dilatant damage resulting from microfracturing that increases permeability and the potential for crack propagation, and by tensile stresses which cause salt fracture and crack propagation. Dilatancy in the salt, caused by excessive shear and deviatoric stresses in comparison with the normal pressure, is evaluated here by the use of the salt damage factor (analogous to a safety factor). This has been developed from a dilatant damage criterion based on a linear function of the hydrostatic pressure [21]. Dilatancy is considered as the onset of damage to rock resulting in significant increases in permeability. Dilatant damage in salt typically occurs at a stress state where a rock reaches its minimum volume, or dilation limit, at which point microfracturing increases the volume. Dilatant criteria typically relate two stress invariants: the mean stress invariant I_1 (equal to three times the average normal stress) and the square root of the stress deviator invariant J_2, or $\sqrt{J_2}$ (a measure of the overall deviatoric or dilatant shear stress). (By convention, tensile normal stresses are positive, and compressive normal stresses are negative, hence the sign nomenclature in the following equations.) Based on the dilatancy criterion from [21], the following damage safety factor has been developed, for which values less than 1.0 indicate the onset of dilatant damage:

$$SF_{VS} = \frac{-0.27I_1}{\sqrt{J_2}} \qquad (1)$$

A quick way to evaluate the potential for damage is by the use of history plots of the extreme values of damage factor and maximum principal stress in the salt surrounding the cavern through each of the five leaching operations. Figure 15 shows the minimum value of the damage factor surrounding several caverns as a function of time through five drawdowns. The lowest values of damage factor occur during workover operation periods. For the vast majority of caverns, the minimum safety factor never decreases below 1.0. One cavern, WH-110, has several periods where at least one point along the cavern wall was found to have values below 1.0, indicating potential dilatant damage. For that cavern, the location of the extreme value was found to be in the cavern floor, which is a location that would not have a detrimental effect on cavern stability. Caverns WH-6 and 9 exhibit significant periods where the damage factor is less than 1.0. These instances are due to their unusual cavern geometries and their close proximity, and are thought to be significant indicators of potential integrity problems. The ramifications of these issues are discussed in the next section. Figure 16 shows a similar plot of the maximum value of the maximum principal stress around selected caverns. In Figure 16, a positive value indicates tensile stress, and therefore the potential for crack formation and propagation. A similar pattern is seen here, as WH-6 and 9 have significant issues, and WH-110 has prominent issues that occur at the cavern floor and are not thought to affect cavern integrity. It has been observed that locations of low damage safety factor and positive tensile stresses are almost always coincident in the same locations.

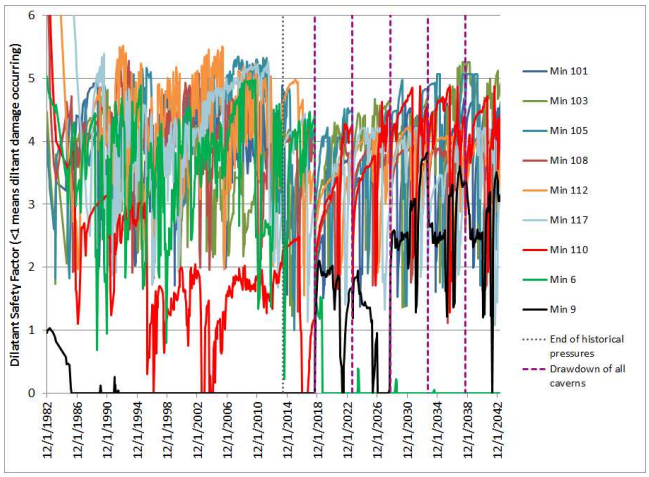

Fig. 15. Minimum value of the damage safety factor surrounding selected caverns.

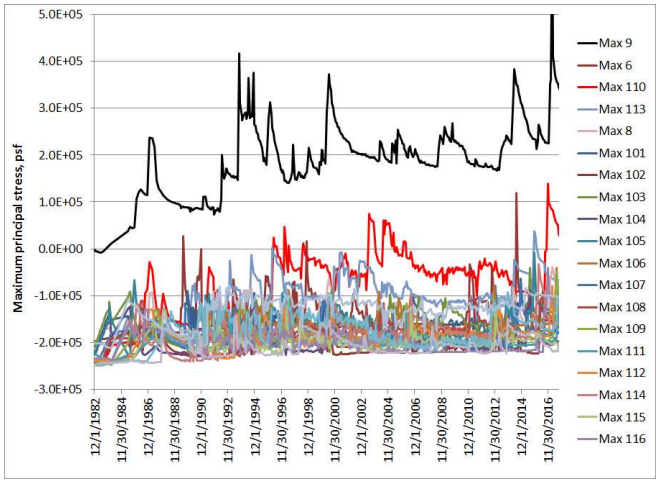

Fig. 16. Maximum value of the maximum principal stress surrounding selected caverns.

6. CAVERNS 6, 8, AND 9

The unusual geometries and close proximity of Caverns WH-6, 8, and 9 present difficult technical issues regarding operations and cavern integrity. Previous papers have analyzed the effects of the large diameter-to-height ratio of Cavern WH-6 on its own potential for cracking around its perimeter, its effect on the stability of nearby WH-9, and the potential inaccessibility of oil due to the large sag in its roof [8-10]. As a result of recommendations based on these papers, the DOE has removed as much oil as possible from WH-6, with the intention of maintaining the cavern as a pressurized brine cavern into the foreseeable future. Caverns WH-8 and WH-9 are also closely located, as illustrated in Figure 17. The locations of primary concern for these two caverns, where dilatant and/or tensile damage are most likely to occur, are the points where the two caverns are in closest proximity: the top of the lower lobe of WH-9 and the bottom of the lower lobe of WH-8. An analysis of the dilatant and normal stresses in these locations indicates that under normal operating conditions, these caverns are expected to maintain cavern integrity. However, during pressure change scenarios such as workover, care must be taken to decrease and increase the pressure more slowly than for normal cavern operations, because the transient creep response of the salt may create extreme stress conditions if the strain rate is too high. Therefore, cavern pressurization recommendations for WH-8 & 9 have been made to DOE similar to those that had been previously made for WH-6: employ a maximum pressurization and depressurization rate of 50 kPa/hr (7.5 psi/hr) for these caverns [22].

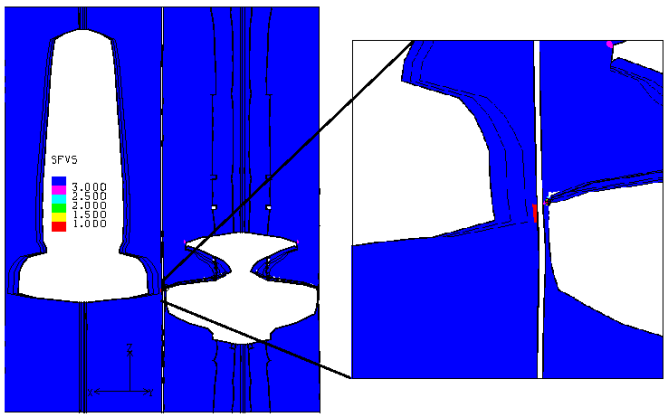

Fig. 17. Maximum value of the maximum principal stress surrounding selected caverns.

7. DRAWDOWN AVAILABILITY

A full drawdown of an oil storage cavern is defined as the removal of 90% of the oil from a cavern with raw water. The addition of raw water to a salt cavern will dissolve salt around the wall, typically adding around 15% to the cavern's volume and decreasing the pillar between that cavern and adjacent caverns. The DOE, in response to requests from the U.S. Congress, wishes to maintain an up-to-date table documenting the number of available full drawdowns of each of the caverns owned by the Strategic Petroleum Reserve. This information is important for assessing the SPR's ability to deliver oil to domestic oil companies expeditiously if national or world events dictate a rapid sale and deployment of the oil reserves. The evaluation of drawdown risks require the consideration of several factors regarding cavern and wellbore integrity and stability, including the ratio of pillar thickness to diameter (P/D) of adjacent caverns, stress states caused by cavern geometry and operations, salt damage caused by dilatant and tensile stresses, the effect on enhanced creep on wellbore integrity, and the sympathetic stress effect of operations on neighboring caverns. The P/D ratio for a cavern with respect to an adjacent cavern is measured by using the minimum distance between points on the walls of the adjacent caverns for the pillar thickness, and the maximum diameter of the cavern in question. For SPR operations, a P/D ratio greater than 1.0 is assumed to represent a condition of good cavern integrity, based on industry and regulatory standards. However, when the P/D < 1.0, geomechanical analysis is required to assess whether stress conditions around the cavern may lead to instability conditions such as salt fracturing, or the increase of salt permeability due to dilatant stresses.

The computational model analyses presented in this paper and in [14] were used to evaluate the maximum number of available drawdowns for each West Hackberry cavern. Two basic assumptions were implemented in this evaluation: one, every cavern must at some time be emptied of oil, meaning a minimum of one drawdown for each cavern (although if integrity issues warrant it, a drawdown might be performed with brine rather than raw water to preserve pillar thickness); two, a maximum of five drawdowns was set, to account for uncertainty in the quality of salt in the pillars between caverns. Four performance indicators were used to evaluate the case for cavern integrity after a drawdown: the minimum safety factor during a workover after a drawdown; the maximum normal stress during that same workover; the effect of successive workovers on the generation of vertical strain in the wellbore casing; and any other relevant available information, such as the number of recorded salt falls in a cavern. As an example for how this evaluation was performed, Cavern WH-101 is used as an example. Figure 18 shows the predicted minimum value for damage safety factor through five cavern drawdowns; at no point does the value become less than 1.0. Figure 19 shows the predicted maximum principal stress around WH-101 through five drawdowns; at no time does the

stress become tensile. Figure 20 shows the generation of average tensile strain along the section of wellbore casing in the salt; the maximum value never exceeds 1.6 millistrains, the accepted threshold for plastic deformation of the steel casing; nor does the strain rate increase alarmingly with successive drawdowns. Finally, WH-101 has had no recorded salt falls during its operation. For these reasons, the estimate for WH-101 based on geomechanical analyses is that this cavern is stable through 5 drawdowns.

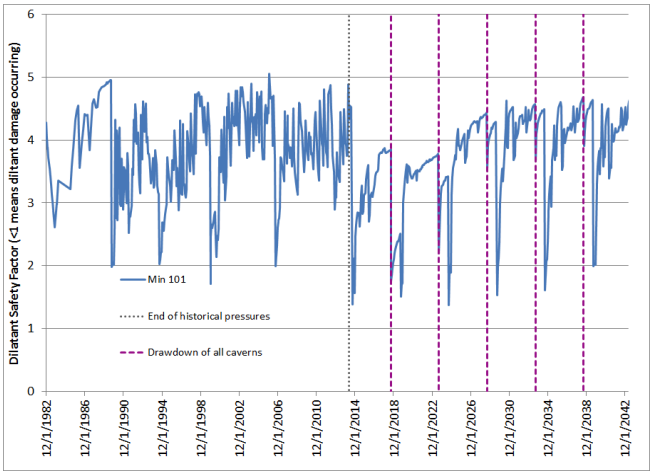

Fig. 18. Minimum value of dilatant safety factor surrounding WH-101.

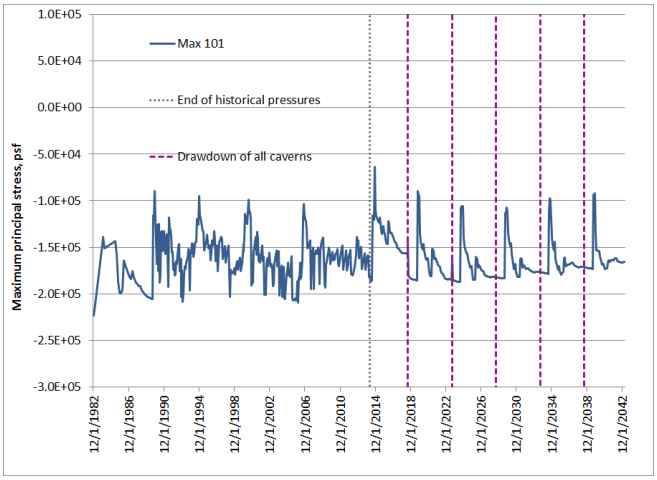

Fig. 19. Maximum value of the maximum principal stress surrounding WH-101.

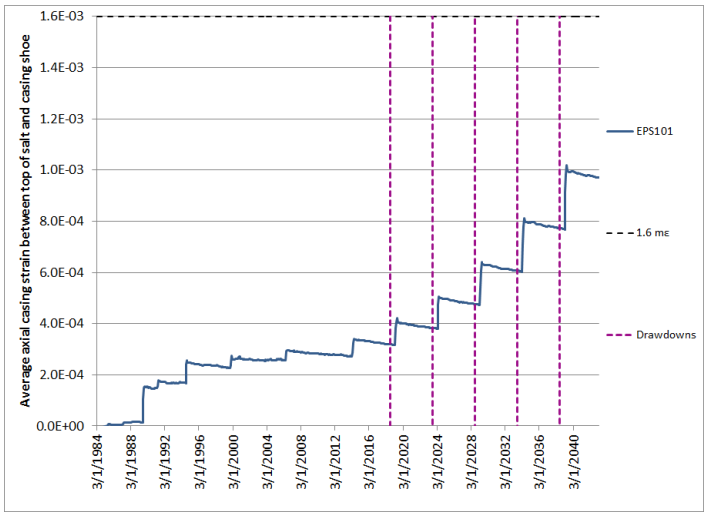

Fig. 20. Predicted avg. axial casing strain between casing shoe and top of salt for WH-101.

A similar evaluation of all the West Hackberry caverns was performed, and all operational oil storage caverns are predicted to be stable through five drawdowns with two exceptions. WH-9 is predicted to have only one remaining drawdown due to the condition that the diameter of its lower lobe cannot be allowed to grow any larger; the combination of proximity to WH-8, and the ledge in the middle of the cavern, are predicted to have a high potential for extreme stress states that would induce cracking. WH-8 is predicted to have a maximum of two drawdowns remaining; the cavern shape is itself mechanically stable, but the proximity to WH-9 raises increases the possibility of a fracture joining the two caverns. This recommendation may be reevaluated if there a desire rises to operate these two caverns as a gallery [23].

8. CONCLUSIONS

The computational model presented in this paper represents a major advancement in the state of the art for geomechanical model of an oil storage facility in domal salt. The advancements include the physical scale of the modeled environment, the number of finite elements in the model, the development of a computational mesh with cavern geometries which fit very closely to sonar measurements of the caverns, the implementation of the M-D creep model, the use of site pressure and subsidence data to develop site and cavern-specific creep properties, and the use of this model to develop long-term cavern operations recommendations for the DOE. The model is now available to use to test out potential operational scenarios for their effect on cavern and wellbore integrity.

9. ACKNOWLEDGEMENTS

Sandia National Laboratories is a multi-program laboratory managed and operated by Sandia Corporation, a wholly owned subsidiary of Lockheed Martin Corporation, for the U.S. Department of Energy's National Nuclear Security Administration under contract DE-AC04-94AL85000.

REFERENCES

1. Preece, D.S. and J.T. Foley, 1984. *Long-Term Performance Predictions for Strategic Petroleum Reserve (SPR) Caverns*, SAND83-2343, Sandia National Laboratories, Albuquerque, New Mexico.

2. Ehgartner, B.L. and S.R. Sobolik, 2002. *3-D Cavern Enlargement Analyses*, SAND2002-0526, Sandia National Laboratories, Albuquerque, New Mexico.

3. Sobolik, S.R. and B.L. Ehgartner, 2009. *Analysis of Cavern Stability at the West Hackberry SPR Site*, SAND2009-2194, Sandia National Laboratories, Albuquerque, New Mexico.

4. Munson, D.E. and P.R. Dawson, 1979. *Constitutive Model for the Low Temperature Creep of Salt (With Application to WIPP).* SAND79-1853, Sandia National Laboratories, Albuquerque, New Mexico.

5. Munson, D.E. and P.R. Dawson. 1982. *A Transient Creep Model for Salt during Stress Loading and Unloading.* SAND82-0962, Sandia National Laboratories, Albuquerque, New Mexico.

6. Munson, D.E. and P.R. Dawson, 1984. Salt Constitutive Modeling using Mechanism Maps. *1st International Conference on the Mechanical Behavior of Salt, Trans Tech Publications*, 717-737, Clausthal, Germany.

7. Sobolik, S.R., J.E. Bean, and B.L. Ehgartner, 2010. Application of the Multi-Mechanism Deformation Model for Three-Dimensional Simulations of Salt Behavior for the Strategic Petroleum Reserve. In *Proceedings of the 44th US Rock Mechanics Symposium and 5th U.S.-Canada Rock Mechanics Symposium, Salt Lake City, UT June 27–30, 2010,* ARMA No. 10-403.

8. Sobolik, S.R. & B.L. Ehgartner, 2012. Analyzing Large Pressure Changes on the Stability of Large-Diameter Caverns Using the M-D Model. In *Mechanical Behavior of Salt VII: Proceedings of the 7th Conference on the Mechanical Behavior of Salt, Paris, France, 16-19 April 2012,* eds. Berest, Ghoreychi, Hadj-hassen & Tijani, 321-330. London: CRC Press, Taylor & Francis Group.

9. Sobolik, S.R. 2013. Analyzing the Effect of Large Pressure Changes on the Operational Stability of Large-Diameter Caverns for the Strategic Petroleum Reserve. In *Proceedings of the 47th US Rock Mechanics Symposium, San Francisco, CA, June 23–26, 2010,* ARMA No. 13-226.

10. Sobolik, S.R. & A.S. Lord, 2015. Operation, Maintenance, and Monitoring of Large-Diameter Caverns in Oil Storage Facilities in Domal Salt. In *Mechanical Behavior of Salt VIII: Proceedings of the 8th Conference on the Mechanical Behavior of Salt, Rapid City, South Dakota, USA, 25-27 May 2015,* eds. Roberts, Mellegard, & Hansen. London: CRC Press, Taylor & Francis Group.

11. Blanford, M.L., M.W. Heinstein, & S.W. Key, 2001. *JAS3D. A Multi-Strategy Iterative Code for Solid Mechanics Analysis. User's Instructions, Release 2.0.* SEACAS Library, JAS3D Manuals, Computational Solid Mechanics / Structural Dynamics, Sandia National Laboratories, Albuquerque, NM.

12. SIERRA Solid Mechanics Team, 2010. *Adagio 4.18 User's Guide.* SAND2010-6313, Sandia National Laboratories, Albuquerque, New Mexico.

13. SIERRA Solid Mechanics Team, 2011. *Sierra/Solid Mechanics 4.22 User's Guide.* SAND2011-7597, Sandia National Laboratories, Albuquerque, New Mexico.

14. Sobolik, S.R., 2015. *Analysis of Cavern and Well Stability at the West Hackberry SPR Site Using a Full-Dome Model*, SAND2015-7401, Sandia National Laboratories, Albuquerque, New Mexico.

15. Weber, P.D., D.K. Rudeen, & D.L. Lord, 2014. *SANSMIC Validation*, SAND2014-16980, Sandia National Laboratories Albuquerque, New Mexico.

16. Whiting, G. H., 1980. *Strategic Petroleum Reserve (SPR): Geological Site Characterization Report, West Hackberry Salt Dome*, SAND80-7131, Sandia National Laboratories Albuquerque, New Mexico.

17. Rautman, C.A., J.S. Stein, and A.C. Snider, 2004. *Conversion of the West Hackberry Geological Site Characterization Report to a Three-Dimensional Model*, SAND2004-3981, Sandia National Laboratories, Albuquerque, New Mexico.

18. Checkai, D., G. Osborne, L. Eldredge, and D. Lord, 2014. Pressure Trending Analysis to Support Cavern Integrity Monitoring at the U.S. Strategic Petroleum Reserve. Solution Mining Research Institute Spring Technical Conference, San Antonio, Texas, May 5-6, 2014.

19. Munson, D.E., 1998. Analysis of Multistage and Other Creep Data for Domal Salts, SAND98-2276, Sandia National Laboratories, Albuquerque, New Mexico.

20. Ballard, S. and B. L. Ehgartner, 2000. *CaveMan Version 3.0: A Software System for SPR Cavern Pressure Analysis*, SAND2000-1751, Sandia National Laboratories, Albuquerque, New Mexico.

21. Van Sambeek, L.L., J.L. Ratigan, & F.D. Hansen, 1993. Dilatancy of Rock Salt in Laboratory Tests, *Int. J. Rock Mech. Min. Sci. & Geomech. Abstr.* Vol. 30, No. 7, 735-738.

22. Sobolik, S.R., 2015. *Sandia Analysis of the Safe Operation Capability of West Hackberry Caverns 8 and*

9 from a Geomechanical Perspective, Letter to Paul Malphurs, DOE-SPR, April 22, 2015.

23. Sobolik, S.R., 2016. *Assessment of the Available Drawdowns for Oil Storage Caverns at the West Hackberry SPR Site*, SAND2016-xxxx (in review at press time), Sandia National Laboratories, Albuquerque, New Mexico.